Charge density on thin straight wire, revisited

J. D. Jackson
University of California, Berkeley, California 94720

(Received 12 November 1999; accepted 11 February 2000)

The question of the equilibrium linear charge density on a charged straight conducting ''wire'' of finite length as its cross-sectional dimension becomes vanishingly small relative to the length is revisited in our didactic presentation. We first consider the wire as the limit of a prolate spheroidal conductor with semi-minor axis a and semi-major axis c when $a/c<<1$. We then treat an azimuthally symmetric straight conductor of length $2c$ and variable radius $r(z)$ whose scale is defined by a parameter a. A procedure is developed to find the linear charge density $\lambda(z)$ as an expansion in powers of $1/\Lambda$, where $\Lambda \equiv \ln(4c^2/a^2)$, beginning with a uniform line charge density λ_0. We show, for this rather general wire, that in the limit $\Lambda>>1$ the linear charge density becomes essentially uniform, but that the tiny nonuniformity (of order $1/\Lambda$) is sufficient to produce a tangential electric field (of order Λ^0) that cancels the zeroth-order field that naively seems to belie equilibrium. We specialize to a right circular cylinder and obtain the linear charge density explicitly, correct to order $1/\Lambda^2$ inclusive, and also the capacitance of a long isolated charged cylinder, a result anticipated in the published literature 37 years ago. The results for the cylinder are compared with published numerical computations. The second-order correction to the charge density is calculated numerically for a sampling of other shapes to show that the details of the distribution for finite $1/\Lambda$ vary with the shape, even though density becomes constant in the limit $\Lambda\to\infty$. We give a second method of finding the charge distribution on the cylinder, one that approximates the charge density by a finite polynomial in z^2 and requires the solution of a coupled set of linear algebraic equations. Perhaps the most striking general observation is that the approach to uniformity as $a/c\to 0$ is extremely slow. © *2000 American Association of Physics Teachers.*

I. INTRODUCTION

In recent years, the question, ''Is the linear charge density on a finite length of a charged straight conducting wire of infinitesimal cross section constant, or even well defined?'' has been addressed in this journal by Griffiths and Li,[1] Good,[2] and Andrews.[3] Although a variety of results are obtained for the equivalent of conductors of small transverse dimension, the focus was on the limit of vanishing lateral extent. All the authors agree that in that exact limit the charge density is uniform. There remains, however, a puzzle, stressed to the present author by Bruce D. Winstein. Figure 1 displays a uniform line charge of length $2c$ parallel to the z axis and centered about $z=0$. Consider an element of charge dq at z. The sum of the electric fields produced by the unshaded segments on either side produces no net force on the element dq, but the shaded segment does. An elementary calculation shows that the force is

$$dF = dq\, E_z = dq\, \frac{\lambda_0}{2\pi\epsilon_0}\, \frac{z}{c^2-z^2}, \tag{1}$$

where λ_0 is the uniform linear charge density. Clearly, dq cannot be in equilibrium!

How can the equilibrium charge distribution on such a conductor be uniform if there are unbalanced forces? One aspect of the problem that might argue for caution is physical. The potential of an isolated finite wire with a fixed amount of charge Q on it grows arbitrarily large as its transverse dimensions decrease, increasing as $Q\ \ln(D/a)$, where $D(a)$ is a distance of the order of the length (transverse dimension) of the wire. In the limit $a\to 0$, the potential becomes infinite unless $Q\to 0$. Conversely, for the practical situation of a wire placed at fixed potential V, the limit $a\to 0$ implies that Q or λ_0 must vanish. With no linear charge density, there is no force! From this point of view, Griffiths and Li[1] were right in their doubts about a valid limit—like the cat in Lewis Carroll's Alice's Adventures in Wonderland, in the limit of $a\to 0$, nothing is left but the grin. This V fixed, $a\to 0$ argument is a red herring, however, as we show below. Physicists never quite go to the limit.

Our paper is aimed at clarifying these issues by focusing on the situation for very large D/a, not the limit $a=0$, although that limit, properly understood, is smooth. The discussion is frankly pedagogical, without much claim of originality. Some aspects are similar in approach to Andrews,[3] others to the much earlier (and actually definitive) work of Vainshtein and colleagues[4–6] and also Waterman.[7]

We first treat the special case of the long straight ''wire'' as the limit of a very elongated prolate spheroidal conductor—special because it has a *uniform linear* charge density, whatever its aspect ratio. In the limit of great elongation, the force (1) applies and is necessary to maintain charge equilibrium, not destroy it! We then examine a ''wire'' consisting of a straight azimuthally symmetric conductor of length $2c$ and possibly variable radius $r(z)$, which is of the order of a transverse scale parameter a. We consider $a/c<<1$, or more correctly, $\Lambda \equiv 2\ln(2c/a)>>1$. In that limit the finishings at the ends of the cylinder and, indeed, whether it is hollow or not, are not significant in determining the charge density over the vast majority of the surface. We show that there are corrections to the uniform charge density of relative magnitude $O(1/\Lambda^n)$ times functions of z/c, for $n=1,2,\ldots$. For most shapes, the additions to the charge density peak toward the ends, as expected, and despite being of order $1/\Lambda$ and smaller, are such that they balance the

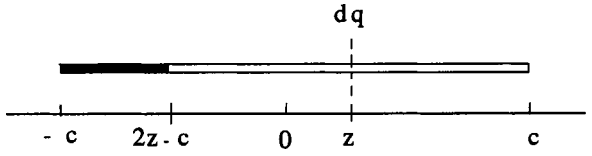

Fig. 1. Line charge of uniform density. The charge of the shaded portion exerts an unbalanced force to the right on dq at z.

Λ-independent force (1) from the dominant uniform linear density to produce electrostatic equilibrium. The appearance of a factor of Λ in the numerator of the force from these additional charge densities, which are of relative order $1/\Lambda$, is what resolves the puzzle of Fig. 1. The tiny nonuniform linear charge density produces a Λ-independent force because some of those charges locally get closer and closer to any observation point as $a/c \to 0$ $(\Lambda \to \infty)$.

The right circular cylinder is treated in detail by two methods (Secs. IV and VI). Examples are given of the charge densities for shapes other than the spheroid and the cylinder, showing that the details of the distribution for wires of small, but not vanishing, radius depend on the shape. The slow approach to uniformity with increasing Λ is also illustrated (Sec. V).

II. CHARGED CONDUCTING PROLATE SPHEROID

A wire as the limiting case of a conducting prolate spheroid has been treated by others. We are brief and only stress the issue of the longitudinal force (1) as a necessary force, not a puzzle. The spheroidal conductor has semi-major and semi-minor axes, c and (a,b) with $b=a$. The equilibrium surface charge density is[8]

$$\sigma(\rho,z)=\frac{Q}{4\pi a^2 c}\,\frac{1}{\sqrt{\dfrac{\rho^2}{a^4}+\dfrac{z^2}{c^4}}}, \tag{2}$$

where Q is the total charge; the spheroid is centered at the origin with the z axis as the major axis, and $\rho^2=x^2+y^2$. It is of interest to find the charge density per unit length dQ/dz. Figure 2 shows the geometry. At the point P the element of area around the circumference of width dz is $dA=2\pi\rho\,dz/\cos(\alpha)$. From the equation of the ellipse $(\rho^2/a^2+z^2/c^2=1)$ and $\tan\alpha=-d\rho/dz$, we find

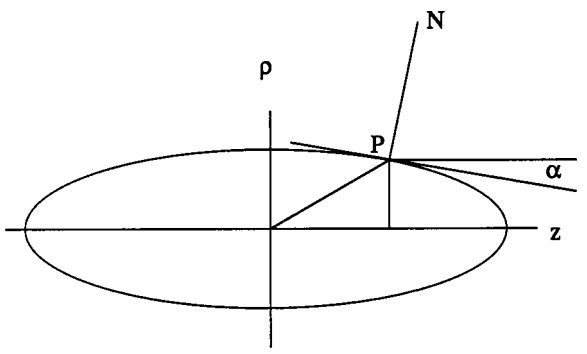

Fig. 2. Geometry of the prolate spheroid for computation of the linear charge density.

$$dA=2\pi a^2\sqrt{\frac{\rho^2}{a^4}+\frac{z^2}{c^4}}\,dz. \tag{3}$$

But $\sigma\,dA=\lambda\,dz$ and because the factor in dA is the reciprocal of the one in $\sigma(\rho,z)$, the charge density per unit length in z is

$$\lambda(z)=\frac{Q}{2c} \tag{4}$$

constant and independent of the ratio of minor to major axis! In the limit of $a/c\to 0^+$, the spheroid goes over automatically to a uniform line of charge with $\lambda_0=Q/2c$.

For a conductor the electric field at the surface is normal to it, with magnitude $|\mathbf{E}|=\sigma/\epsilon_0$. The components of the electric field at the surface may therefore be computed from the surface charge density and the angle α: $E_z=(\sigma/\epsilon_0)\sin\alpha$ and $E_\rho=(\sigma/\epsilon_0)\cos\alpha$. We need

$$\cos\alpha=\frac{\sqrt{c^2-z^2}}{\sqrt{c^2-(1-a^2/c^2)z^2}},\qquad \sin\alpha=\frac{az}{c\sqrt{c^2-(1-a^2/c^2)z^2}}, \tag{5}$$

where we have used the equation of the ellipse to give expressions as functions of z alone. Note that, to first order in a/c, $\cos\alpha\approx 1$ and $\sin\alpha\approx az/c(c^2-z^2)^{1/2}$; the normal to the surface (PN in Fig. 2) is almost radial, with only a small component in the axial direction. In that limit, however, the magnitude of the electric field is huge. Explicitly, the components of the electric field at the surface of the spheroid for arbitrary a/c are

$$E_z=\frac{\lambda_0}{2\pi\epsilon_0}\,\frac{z}{[c^2-(1-a^2/c^2)z^2]},\qquad E_\rho=\frac{\lambda_0 c}{2\pi\epsilon_0 a}\,\frac{\sqrt{c^2-z^2}}{[c^2-(1-a^2/c^2)z^2]}. \tag{6}$$

In the limit $a^2/c^2<<1$, these expressions reduce to

$$E_z=\frac{\lambda_0}{2\pi\epsilon_0}\,\frac{z}{[c^2-z^2]},\qquad E_\rho=\frac{\lambda_0 c}{2\pi\epsilon_0 a\sqrt{c^2-z^2}}=\frac{\lambda_0}{2\pi\epsilon_0\rho(z)}. \tag{7}$$

The axial component is independent of a in the limit $a^2/c^2<<1$ and agrees with dF/dq from Eq. (1). It results from the product of an infinite surface charge density $(\sigma\propto 1/a)$ and a vanishing $\sin\alpha(\propto a)$. The radial component of the electric field in the limit is just the naive result obtained by applying Gauss's law around the ''wire.'' It grows without limit as $a/c\to 0+$, except at the very ends [where (6), not (7), must be used].

The elongated prolate spheroid specifies one limiting form of a finite ''wire'' of negligible cross section. It is special in that its charge density per unit length is constant, independent of the ratio a/c. For such a uniform charge density, the argument of Sec. I shows that in the limit of $a/c\to 0+$ there must be an axial electric field E_z given by (1) or (7). Con-

trary to the discussion there, however, we see here that the axial field is required to guarantee that the charge be in equilibrium on the spheroidal surface.

Obviously the spheroidal wire is a very special case, but not the only one. As shown by Griffiths and Li,[1] for the *general ellipsoidal conductor* with arbitrary values of the principal axes $(2a,2b,2c)$, the linear charge density along a principal axis is constant and given by (4), if the third axis is the chosen one. In the limit $a<<b<<c$, the ellipsoid approximates in a special way a flattened wire. We now turn to a more general (but cylindrically symmetric) shape.

III. GENERAL AZIMUTHALLY SYMMETRIC CONDUCTING CYLINDER

A. Linear charge density to order $1/\Lambda^2$ inclusive

Consider our ''wire'' to be a long, thin, straight, azimuthally symmetric conductor of length $2c$ and possibly variable radius $r(z)$, whose scale is set by the radial parameter a, with $a/c<<1$. In fact, the criterion for long and thin is more stringent, namely, $\Lambda\equiv 2\ln(2c/a)>>1$. Specifically, we choose

$$[r(z)]^2=a^2 f(z), \tag{8}$$

where $f(z)$ is a smooth positive function, of order unity and bounded above and below for $|z|<c$, and vanishing at $|z|=c$. Later, we specialize to $f(z)=(1-|z/c|)^2$ and $f(z)=1-|z/c|^n$, with n a positive even integer.

We approach the problem of finding the equilibrium linear charge density on the surface of the conductor through the potential of a line charge (zero cylinder radius) evaluated at $\rho=r(z)$ and beyond, as did Andrews.[3] We develop a systematic iterative scheme to find the charge density as a power series in $1/\Lambda$, beginning with the lowest order approximation, a line charge of constant density λ_0 extending over the range $-c<z<c$. Straightforward integration shows that the electrostatic potential is

$$\Phi^{(0)}(\rho,z)=\frac{\lambda_0}{4\pi\epsilon_0}\int_{-c}^{c}\frac{dz'}{\sqrt{\rho^2+(z'-z)^2}}=\frac{\lambda_0}{4\pi\epsilon_0}\ln\left[\frac{z+c+\sqrt{\rho^2+(z+c)^2}}{z-c+\sqrt{\rho^2+(z-c)^2}}\right]. \tag{9}$$

We are interested in the potential near the wire $[\rho\approx O(a)<<c,|z|<c]$. Introducing the scaled variable $\zeta\equiv z/c$, and expanding the argument of the logarithm to first order in $(\rho/c)^2$, we find the potential can be approximated by

$$\Phi^{(0)}(\rho,z)=\frac{\lambda_0\Lambda}{4\pi\epsilon_0}\left[1+\frac{1}{\Lambda}\ln(1-\zeta^2)+\frac{1}{\Lambda}\ln(a^2/\rho^2)+\frac{(\rho^2/c^2)(1+\zeta^2)}{2\Lambda(1-\zeta^2)^2}+\cdots\right] \tag{10}$$

provided the observation point is not too close to the ends. The last term can be neglected provided $[1-|\zeta|]>>\rho/2c$, a condition satisfied over most of the wire provided $\Lambda>>1$. Using (8) and omitting the last term in (10), we have the approximate but accurate expression

$$\Phi^{(0)}(\rho,z)=\frac{\lambda_0\Lambda}{4\pi\epsilon_0}\left[1+\frac{1}{\Lambda}\ln\left(\frac{1-\zeta^2}{f(\zeta)}\right)+\frac{1}{\Lambda}\ln(r^2(\zeta)/\rho^2)\right]. \tag{11}$$

The integral in (9) is large, equal to Λ in leading order, because of a peaking of the integrand at $z'=z$, but with z/c- *and* $\rho/r(\zeta)$-dependent terms in next order. From (11) we see that, beyond the leading order, the potential is not constant on the surface of the conductor, $\rho=r(\zeta)$.

We wish to find an addition $\lambda_1(z)$ to the constant linear charge density λ_0 such that its potential, when added to (11), will remove the ζ dependence at $\rho=r(\zeta)$ and give an equipotential conductor. Evidently, λ_1/λ_0 will be of order $1/\Lambda$. To this end, consider the potential $\Phi^{(1)}(\rho,z)$ produced by $\lambda_1(z)$:

$$\Phi^{(1)}(\rho,z)=\frac{1}{4\pi\epsilon_0}\int_{-c}^{c}\frac{\lambda_1(z')dz'}{\sqrt{\rho^2+(z'-z)^2}}. \tag{12}$$

We add and subtract $\lambda_1(z)$ to the numerator and write

$$\Phi^{(1)}(\rho,z)=\frac{\lambda_1(z)}{4\pi\epsilon_0}\int_{-c}^{c}\frac{dz'}{\sqrt{\rho^2+(z'-z)^2}}+\frac{1}{4\pi\epsilon_0}\int_{-c}^{c}\frac{[\lambda_1(z')-\lambda_1(z)]dz'}{\sqrt{\rho^2+(z'-z)^2}}.$$

The first integral is proportional to $\Phi^{(0)}$ given by (11). The second integral has an integrand that is unexceptional near $z'=z$ because the numerator vanishes there. In fact, in the limit of $\Lambda>>1$, we may set $\rho=0$ in the denominator with the introduction of errors only of the order of ρ^2/c^2. We thus have

$$\Phi^{(1)}(\rho,z)=\frac{\lambda_1(z)}{\lambda_0}\Phi^{(0)}(\rho,z)+\frac{1}{4\pi\epsilon_0}\int_{-c}^{c}\frac{[\lambda_1(z')-\lambda_1(z)]dz'}{|z'-z|}. \tag{13}$$

The leading contribution to the first term in (13) is Λ [times $\lambda_1(z)/4\pi\epsilon_0$], while the second integral and the remainder of the first term is, as observed by Andrews,[3] of lower order in Λ. Focusing on the leading order part of $\Phi^{(1)}$ [because it is already down by one power of Λ and so of the same order as the second and third terms in (11)], we have the sum of $\Phi^{(0)}$ and $\Phi^{(1)}$, evaluated on the cylinder $[\rho=r(\zeta)]$ as

$$\Phi^{(0)}(r(z),z)+\Phi^{(1)}(r(z),z)\approx\frac{\lambda_0\Lambda}{4\pi\epsilon_0}\left[1+\frac{1}{\Lambda}\ln\left(\frac{1-\zeta^2}{f(\zeta)}\right)+\frac{\lambda_1(z)}{\lambda_0}\right]. \tag{14}$$

To assure constancy of the sum to order $1/\Lambda$ inclusive, the first-order correction to the charge density must be

$$\frac{\lambda_1(z)}{\lambda_0}=-\frac{1}{\Lambda}\ln\left(\frac{1-\zeta^2}{f(\zeta)}\right). \tag{15}$$

The complete linear charge density, correct to first order in $1/\Lambda$, is then

$$\lambda^{(1)}(z)=\lambda_0\left[1-\frac{1}{\Lambda}\ln\left(\frac{1-\zeta^2}{f(\zeta)}\right)\right]. \tag{16}$$

This expression is equivalent to the approximation asserted by Andrews[3] [his Eq. (3.2), in my notation]

$$\lambda_{\text{Andrews}}(z)=\frac{\lambda_0}{1+\frac{1}{\Lambda}\ln\left(\frac{1-\zeta^2}{f(\zeta)}\right)}. \tag{16'}$$

For use below, we note in passing the result for the *leading order* part of $\Phi^{(1)}(\rho,z)$:

$$\Phi^{(1)}(\rho,z)\approx-\frac{\lambda_0}{4\pi\epsilon_0}\ln\left(\frac{1-\zeta^2}{f(\zeta)}\right)+O(1/\Lambda). \tag{17}$$

With $\lambda_1(z)$ known, we can proceed to the next step in our iteration scheme. With (15) substituted for $\lambda_1(z)/\lambda_0$, the potential (13), correct to second order in $1/\Lambda$, is explicitly

$$\begin{aligned}\Phi^{(0)}(\rho,z)+\Phi^{(1)}(\rho,z)&\\ =\frac{\lambda_0\Lambda}{4\pi\epsilon_0}\Bigg\{1-\frac{1}{\Lambda^2}\left[\ln\left(\frac{1-\zeta^2}{f(\zeta)}\right)\right]^2+\frac{1}{\Lambda^2}I&\\ +\frac{1}{\Lambda}\ln\left(\frac{r^2(\zeta)}{\rho^2}\right)\left[1-\frac{1}{\Lambda}\ln\left(\frac{1-\zeta^2}{f(\zeta)}\right)\right]\Bigg\},&\end{aligned} \tag{18}$$

where the integral I, of order unity despite appearances, is

$$\begin{aligned}I&=\frac{\Lambda}{\lambda_0}\int_{-1}^{1}\frac{dx}{|x-\zeta|}[\lambda_1(x)-\lambda_1(\zeta)]\\ &=\int_{-1}^{1}\frac{dx}{|x-\zeta|}\left[\ln\left(\frac{1-\zeta^2}{f(\zeta)}\right)-\ln\left(\frac{1-x^2}{f(x)}\right)\right].\end{aligned} \tag{19}$$

The $1/\Lambda$ term at $\rho=r(\zeta)$, present in $\Phi^{(0)}$, has been eliminated by λ_1, leaving a second-order variation in z. By the same steps from (12) to (14) with a $\lambda_2(z)$ instead of λ_1, we can infer that the first line in (18) is the negative of the charge density $\lambda_2(z)/\lambda_0$. The linear charge density, correct to order $1/\Lambda^2$ inclusive, is therefore

$$\lambda(\zeta)=\lambda_0\left\{1-\frac{1}{\Lambda}\ln\left(\frac{1-\zeta^2}{f(\zeta)}\right)+\frac{1}{\Lambda^2}\left[\left[\ln\left(\frac{1-\zeta^2}{f(\zeta)}\right)\right]^2-I\right]\right\}. \tag{20}$$

The scheme of iteration is now clear. The second-order charge density $\lambda_2(z)$ can be inserted into (13) instead of $\lambda_1(z)$ to generate $\Phi^{(2)}(\rho,z)$. The sum of potentials will then be constant up to order $1/\Lambda^2$, but will have z-dependent terms of order $1/\Lambda^3$. These can be removed by identifying $\lambda_3(z)$, and so on. In higher order, however, the integrals equivalent to I become intractable in terms of known functions. Even (19) needs numerical computation, except for special choices of $f(z)$.

Before evaluating (19) and (20) for specific shapes for $f(z)$, we address the conundrum posed in Sec. I. In Sec. II we saw how the puzzle was not actually a puzzle but a necessity for the spheroidal shape. But what about other shapes?

B. General resolution of the issue of the axial electric field and charge equilibrium

Because of the shape of the conductor, defined by $r(z)$ in (8), care must be taken to distinguish between the electric field in the z direction and the electric field tangential to the surface in the $\rho-z$ plane. If β is the angle between the tangent vector and the z axis in that plane, its tangent is $\tan\beta=dr(z)/dz=r'(\zeta)/c$, where $r'(\zeta)=dr/d\zeta$. Define the scale of variation of $r(z)$ to be $O(b)$, with $a<<b$. Then $r'=O(ac/b)$ and $\tan\beta=O(a/b)<<1$. We therefore have $\sin\beta\approx r'/c$ and $\cos\beta\approx1$, with corrections of order (a^2/b^2). The components of the zeroth-order electric field in the z and ρ directions at the surface are, from (10) or (11),

$$\begin{aligned}E_z^{(0)}&=-\frac{\partial\Phi^{(0)}}{c\,\partial\zeta}=\frac{\lambda_0}{2\pi\epsilon_0 c}\left(\frac{\zeta}{1-\zeta^2}\right),\\ E_\rho^{(0)}&=-\frac{\partial\Phi^{(0)}}{\partial\rho}=\frac{\lambda_0}{2\pi\epsilon_0 c}\left(\frac{c}{r(\zeta)}\right).\end{aligned} \tag{21}$$

The zeroth-order component of the electric field tangential to the surface is

$$\begin{aligned}E_{\tan}^{(0)}&=E_z^{(0)}\cos\beta+E_\rho^{(0)}\sin\beta\\ &=\frac{\lambda_0}{4\pi\epsilon_0 c}\left[\frac{2\zeta}{1-\zeta^2}+\frac{2r'}{r}\right]\\ &=-\frac{\lambda_0}{4\pi\epsilon_0 c}\frac{d}{d\zeta}\ln\left(\frac{1-\zeta^2}{f(\zeta)}\right).\end{aligned} \tag{22}$$

The first-order potential is given in leading order by (17). It has only a z component of electric field. With $\cos\beta\approx1$, the tangential and z components of the first-order electric field are equal and are

$$E_z^{(1)}=E_{\tan}^{(1)}=-\frac{d\Phi^{(1)}}{c\,d\zeta}=\frac{\lambda_0}{4\pi\epsilon_0 c}\frac{d}{d\zeta}\ln\left(\frac{1-\zeta^2}{f(\zeta)}\right). \tag{23}$$

Comparison of (22) and (23) shows that the lowest order and first-order tangential fields cancel, as they must if the surface is an equipotential. The reader may think this point is a bit of a straw man because the sum of the zeroth- and first-order potentials, shown in (18), is constant on the surface to order $1/\Lambda$, and so must give vanishing tangential electric field to that order. More interesting is the sum of the z components of the electric field,

$$E_z^{(0)}+E_z^{(1)}=-\frac{\lambda_0}{4\pi\epsilon_0 c}\frac{d}{d\zeta}\ln(f(\zeta)). \tag{24}$$

Depending on the form of $f(\zeta)$, there is a nonvanishing *axial* electric field of order Λ^0, but no tangential electric field.

Three points are to be made, as follows.

(1) If the surface is the spheroid of Sec. II, $f(\zeta)=1-\zeta^2$. Then the electric field in the z direction (24) is just (1). Actually, by looking back at (15) and (17), the reader will see that $\lambda_1=0$ and so $\Phi^{(1)}=0$. In this case there are no corrections to the constant linear charge density, as we already know from Sec. II.

(2) For any shape other than the spheroid, the linear charge density has nonvanishing z-dependent corrections that can be written as an expansion in powers of $1/\Lambda$. The example of the second-order linear charge density for the right circular cylinder is considered explicitly in Secs. IV and VI. The second-order charge densities for a family of shapes are discussed briefly in Sec. V.

(3) For a general shape, the zeroth-order constant charge density λ_0 generates a potential $\Phi^{(0)}$, which is constant on the conductor to order Λ plus corrections of order Λ^0. These order Λ^0 terms give rise to the electric field $\mathbf{E}^{(0)}$ whose components are given by (21). The first-order charge density

$\lambda_1(z)$, which is of order $1/\Lambda$, generates a potential $\Phi^{(1)}$ of order Λ^0. The electric field $\mathbf{E}^{(1)}$ is thus of the same order as $\mathbf{E}^{(0)}$ and is such as to combine with it to give a vanishing tangential component of field on the surface. Equilibrium of the surface charge is assured, even in the limit that $1/\Lambda \to 0$, as the charge density approaches uniformity. It is the fact that a nonuniform linear charge density of order Λ^k causes a potential of order Λ^{k+1} that resolves the puzzle posed in Sec. I. Physically, the increase by one in the powers of Λ is a result of the greater and greater peaking of the integrands in the expressions for the potential or the electric field as $a/c \to 0$, the result of contributions from the nonuniform charge density in the immediate neighborhood of the observation point.

IV. RIGHT CIRCULAR CYLINDRICAL CONDUCTOR (1)

A. Charge density to order $1/\Lambda^2$ inclusive

For a right circular cylinder, the radial function $f(z)=1$ for $|z|<c$. Then the integral I (19) is

$$I_{\text{cylinder}} = \int_{-1}^{1} \frac{dx}{|x-\zeta|} [\ln(1-\zeta^2) - \ln(1-x^2)]. \tag{25}$$

We change variables to $t=x-\zeta$, break up the integration into $t<0$ and $t>0$, write out the logs as the sum of four terms and then recombine so that the arguments are linear in t, and finally rescale t to obtain

$$\begin{aligned} I_{\text{cylinder}} = & -2\int_0^1 \frac{du}{u}\ln(1-u) \\ & - \int_0^{(1+\zeta)/(1-\zeta)} \frac{du}{u}\ln(1+u) \\ & - \int_0^{(1-\zeta)/(1+\zeta)} \frac{du}{u}\ln(1+u). \end{aligned}$$

We now break up the second integral into intervals (0, 1) and $(1,(1+\zeta)/(1-\zeta))$. Then in the second part we change variables $u \to 1/u$ to find

$$I_{\text{cylinder}} = -\int_0^1 \frac{dv}{v}\ln(1-v) + \int_{(1-\zeta)/(1+\zeta)}^1 \frac{du}{u}\ln u,$$

where $v=u^2$. The first integral can be found in the tables to be $-\pi^2/6$. The second integral is elementary. The result is

$$I = \frac{\pi^2}{6} - \frac{1}{2}\left[\ln\left(\frac{1+\zeta}{1-\zeta}\right)\right]^2.$$

This gives the linear charge density, correct to order $1/\Lambda^2$ inclusive,

$$\begin{aligned} \lambda(\zeta) = \lambda_0 \Bigg\{ & 1 - \frac{1}{\Lambda}\ln(1-\zeta^2) + \frac{1}{\Lambda^2}\Bigg[[\ln(1-\zeta^2)]^2 \\ & + \frac{1}{2}\left[\ln\left(\frac{1+\zeta}{1-\zeta}\right)\right]^2 - \frac{\pi^2}{6}\Bigg] + O(1/\Lambda^3)\Bigg\} \end{aligned} \tag{26}$$

and the potential near the wire to the same relative order (including $\Phi^{(2)}$) is

$$\Phi(\rho,z) = \frac{\lambda_0\Lambda}{4\pi\epsilon_0}\left[1 + \frac{1}{\Lambda}\frac{\lambda(\zeta)}{\lambda_0}\ln(a^2/\rho^2) + O(1/\Lambda^3)\right]. \tag{27}$$

On the cylinder ($\rho=a$) the potential is constant to order $1/\Lambda^2$ inclusive. Note that, even though $\lambda(\zeta)$ is, strictly speaking, a line charge on the axis ($\rho=0$), the potential (27) for $\rho \geqslant a$ corresponds to a conducting cylinder at $\rho=a$ with the expected surface charge density (computed from the radial electric field) equal to $\lambda(\zeta)/2\pi a$. It can be shown that the difference is of order $a^2/c^2\Lambda^{-1} = O(e^{-\Lambda}/\Lambda)$, with, however, ζ dependence singular as $(1-\zeta^2)^{-n}$ near the ends.

A referee has pointed out that an alternative expression for $\lambda(z)$, yielding the same result as (26) to order $1/\Lambda^2$, is

$$\lambda(\zeta) = \frac{\lambda_0}{\left[1 + \frac{1}{\Lambda}\ln(1-\zeta^2)\right]}\left\{1 + \frac{1}{2\Lambda^2}\left[\left(\ln\left(\frac{1+\zeta}{1-\zeta}\right)\right)^2 - \frac{\pi^2}{3}\right]\right\}. \tag{26$'$}$$

This result combines Andrews' form of the first-order charge density (16′) with the second-order term $-I_{\text{cylinder}}$. Empirically, (26′) is a better approximation to the charge density than (26) in that it keeps the potential on the surface $\rho=a$ an equipotential slightly closer to the ends of the cylinder. The differences disappear rapidly as Λ increases, of course. Our expansion in inverse powers of Λ has advantages in analytic work, in the calculation of the capacitance of the cylinder, for example, see Sec. IV C.

B. Practicalities, comparison with numerical calculations of others

The range of Λ values for practical situations can be judged by considering the range of radii for the largest and smallest diameter copper wires in the American Wire Gauge table: $a=5.842$ mm (AWG No. 0000) to $a=3.993 \times 10^{-2}$ mm (AWG No. 40). For a wire 1 m in length, the range is $\Lambda \approx 10 \to 20$. Finer or longer wires can be imagined, but $\Lambda \leqslant 25$ is a likely upper limit for an isolated wire [if indeed anyone was interested in verifying (26)].

Some numerical calculations exist for the charge density on a cylinder.[5,9,10] Sakar and Rao[9] give a few values for the density for $\Lambda=13.82$. Their numbers are compared with (26) in the top half of Fig. 3. Their averaging interval $\Delta\zeta=2/9$ is sufficiently great that for their largest interval $(7/9<\zeta<1)$ we have used (26) to find a weighted mean position for their point. The agreement is satisfactory. Waterman and Pedersen[10] are concerned with scattering of electromagnetic waves by conducting cylinders, but in an appendix present an empirical parametrization of their numerical results for the charge density for a constant potential along the cylinder. My version of their fit to a range of $\Lambda \approx 15 \to 185$ is $\lambda(\zeta) = \lambda_0(1-\zeta^2)^{-\gamma}$, where $\gamma = 1/(\Lambda-\beta)$ and $\beta \approx 3.025$. For $\Lambda = 15$, this empirical fit is compared with (26) in the bottom half of Fig. 3. The agreements for other values of Λ are comparably good.

Griffiths and Li[1] give a numerical fit [their Eq. (3.7)] to the smoothed charge density of their discrete distribution of 200 point charges on a line. While not strictly comparable to (26), the fit might naively be expected to correspond to $c/a \approx 100-200$ or $\Lambda \approx 10.6-12$. In fact, good agreement of (26) with their formula occurs for $\Lambda \approx 17 \pm 1$.

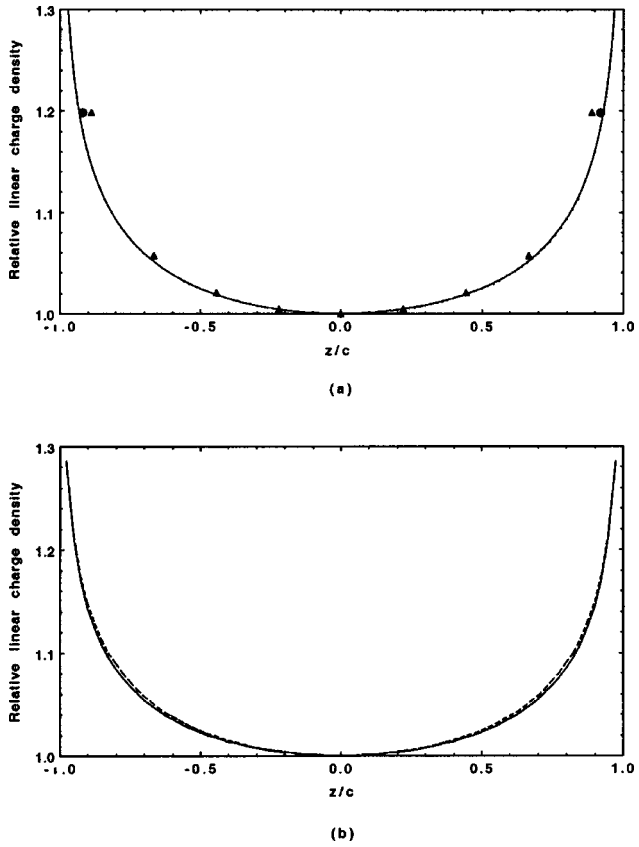

Fig. 3. Comparison of Eq. (26), normalized to unity at $z=0$, with numerical calculations. (a) Sakar and Rao (Ref. 9), $\Lambda=13.82$ (solid triangles; solid dot is mean position weighted according to the shape of (26)). (b) Waterman and Pedersen (Ref. 10), $\Lambda=15$ (dashed curve is empirical fit to their numerical results; see text). Note the suppressed zero for the ordinates.

Despite the peaking at the ends displayed in Fig. 3, the magnitude of the charge density variation is such that the departure from uniformity is rather small. A measure of the nonuniformity is the percentages of charge on the inner half of the cylinder ($|\zeta|<1/2$) and the outer half ($1/2<|\zeta|<1$). For $\Lambda=6$ ($c/a\approx 10$), the percentages are 43% (inner) and 57% (outer). For $\Lambda=20$ ($c/a\approx 1.1\times 10^4$), they are 48% (inner) and 52% (outer).

C. Capacitance of conducting right circular cylinder

The capacitance of an isolated long right circular conducting cylinder of radius a and length $2c$ is found from (26) and (27). From (27) we see that the potential of the cylinder is $V=\lambda_0\Lambda/4\pi\epsilon_0$. The total charge Q is the twice the integral of (26) over the interval, $0<z<c$. The capacitance is therefore

$$C=4\pi\epsilon_0\frac{2c}{\Lambda}\int_0^1\frac{\lambda(\zeta)}{\lambda_0}d\zeta. \tag{28}$$

The result of the integration is

$$C=4\pi\epsilon_0\frac{2c}{\Lambda}\left\{1+\frac{2}{\Lambda}(1-\ln 2)+\frac{4}{\Lambda^2}\left[1+(1-\ln 2)^2-\frac{\pi^2}{12}\right]+O(1/\Lambda^3)\right\} \tag{29}$$

or, numerically,

$$C=4\pi\epsilon_0\frac{2c}{\Lambda}\left\{1+\frac{0.613\,705\,6}{\Lambda}+\frac{1.086\,766}{\Lambda^2}+O(1/\Lambda^3)\right\}.$$

The result (29) is not new. An expression equivalent to it was published by Vainshtein[6] in 1962. He chooses to define $\Omega=\Lambda-2(1-\ln 2)$ to suppress formally the term in $1/\Lambda$ in (29). His form, equivalent to (29), is

$$C=4\pi\epsilon_0\frac{2c}{\Omega}\left\{1+\frac{4-\pi^2/3}{\Omega^2}+O(1/\Omega^3)\right\}. \tag{30}$$

Obviously, Vainshtein derived the charge density, too, but he does not state it explicitly.

The problem of the capacitance of a right circular cylinder has been treated in the literature by numerical methods.[11,12] Smythe[11] used an approximation technique (described in Ref. 8, pp. 209–211) to find the capacitance for $c/a=1,2,4,8$. He gives a convenient interpolation formula, $C/4\pi\epsilon_0 a=2/\pi+0.5539\,(c/a)^{0.7587}$. (The coefficients are from my fit to his numerical values and differ slightly from his.) How does our (Vainshtein's) formula for long cylinders compare with Smythe's? For $c/a=4$ ($\Lambda\approx 4.16$) the values are $C/4\pi\epsilon_0 a=2.328$ [Eq. (29)], 2.222 (Smythe). For $c/a=8$ ($\Lambda\approx 5.545$), they are $C/4\pi\epsilon_0 a=3.307$ [Eq. (29)], 3.320 (Smythe). The fractional errors of (29) compared with Smythe's values are 4.8% and 0.4% for $c/a=4$ and 8, respectively. Vainshtein's version (30) is marginally poorer. It appears that (29) accurately represents the capacitance of a long right circular cylinder for $c/a\geqslant 10$. Smythe's interpolation formula suffices for $0<c/a<10$.

V. SECOND-ORDER LINEAR CHARGE DENSITIES FOR OTHER SHAPES

The second-order linear charge density for a right circular cylinder was expressible in terms of known functions. In general, a random choice of the radial profile $f(\zeta)$ in (19) to compute I will not result in known functions. However, as remarked earlier, the integrand in (19) is quite smooth in its behavior at $x\to\zeta$ (with opposite limits from above and below because of the denominator). It is only necessary to break the integral up into two ranges, $(-1<x<\zeta)$ and $(\zeta<x<1)$, for numerical integration.

Numerical computations of I were done for $f(\zeta)=(1-|\zeta|)^2$, and $f(\zeta)=1-|\zeta|^n$, with n an even integer. The first choice is a ''double cone'' conductor, shown at the top of Fig. 4(a), along with profiles for the second choice of $f(\zeta)$ with $n=2$, 4, 6, 8, and 10. Note that in the limit $n>>2$ the shape of the ''wire'' approximates a right circular cylinder. For $\Lambda=15$, the curves of the second-order charge densities for the double cone and $n=2,4,6,8$ are shown, along with that of the right circular cylinder in Fig. 4(b). The trend from $n=2$ (spheroid) to $n=8$ shows the progression toward the right circular cylinder. In contrast, the double cone conductor has a linear charge density that seems to tend toward zero at the ends. The known behavior of the surface charge density near the tip of a cone (Ref. 13, p. 106) corresponds here to the *linear* charge density $\lambda(\zeta)\propto(1-\zeta)^{1/\Lambda}$. The behavior shown in Fig. 4(b) agrees qualitatively with this dependence, but our results cannot be trusted too close to the ends of the conductor. At $z=0$ the double cone has a discontinuity in slope. The behavior at such places can be deduced from two-

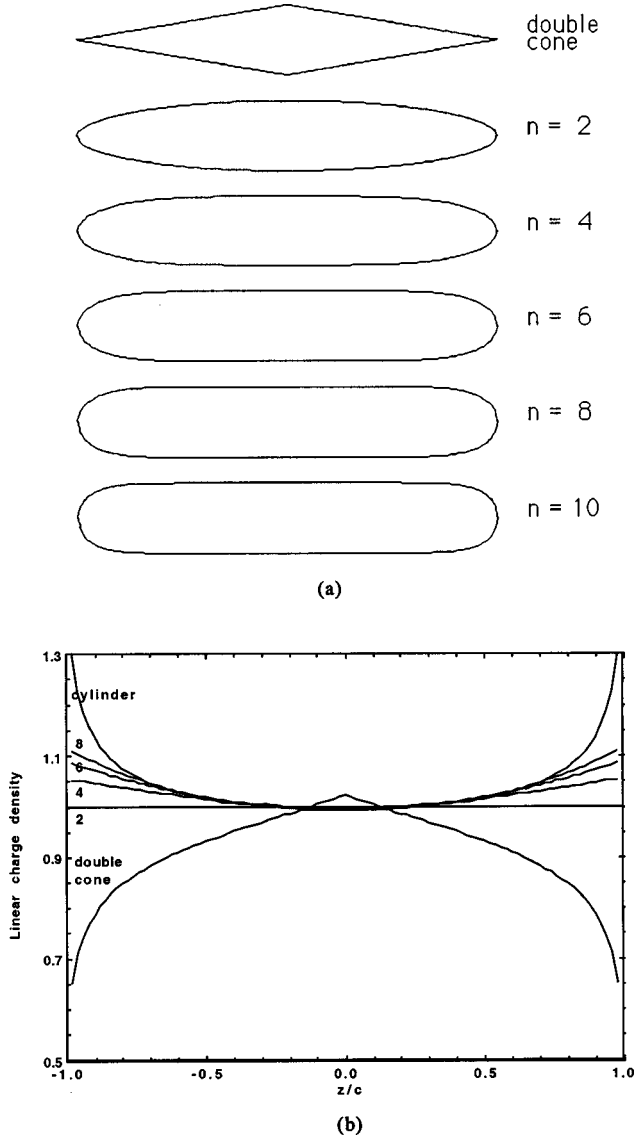

Fig. 4. (a) Shapes of conductors defined by $r(z)/a=1-|z/c|$ [double cone] and $r(z)^2/a^2=1-|z/c|^n$. The transverse (radial) coordinate has been scaled by a factor of $c/6a$ to make the different shapes visible. (b) Linear charge densities for the shapes of part (a) for the double cone and $n=2,4,6,8$ for $\Lambda=15$, along with that of a right circular cylinder. Note the suppressed zero for the ordinate.

dimensional electrostatics (Ref. 13, p. 78). The linear charge density should be singular as $|z|^{-2a/\pi c}$ for $|z|<a$. For $\Lambda=15$, the exponent has absolute value 7×10^{-4}; the singularity is too small in magnitude and extent to be discernible in our numerical integration. In Fig. 5 we display the linear charge densities for the right circular cylinder and for the double cone for $\Lambda=15$, 30, and 60 to illustrate the trend toward uniformity with increasing Λ. The lesson to be learned from Figs. 4 and 5 is that the detailed behavior of the charge density is shape dependent, even for very thin wires. Only in the limit $1/\Lambda=0$, unattainable in practice, where it is approached very slowly, do the differences among conductors absolutely disappear. Even then, the shape-dependent z component of electric field (24) is present! Each cat does have a grin that betrays its identity!

Perturbations around a smooth shape can also be treated, but this would take us too far away from our purpose.

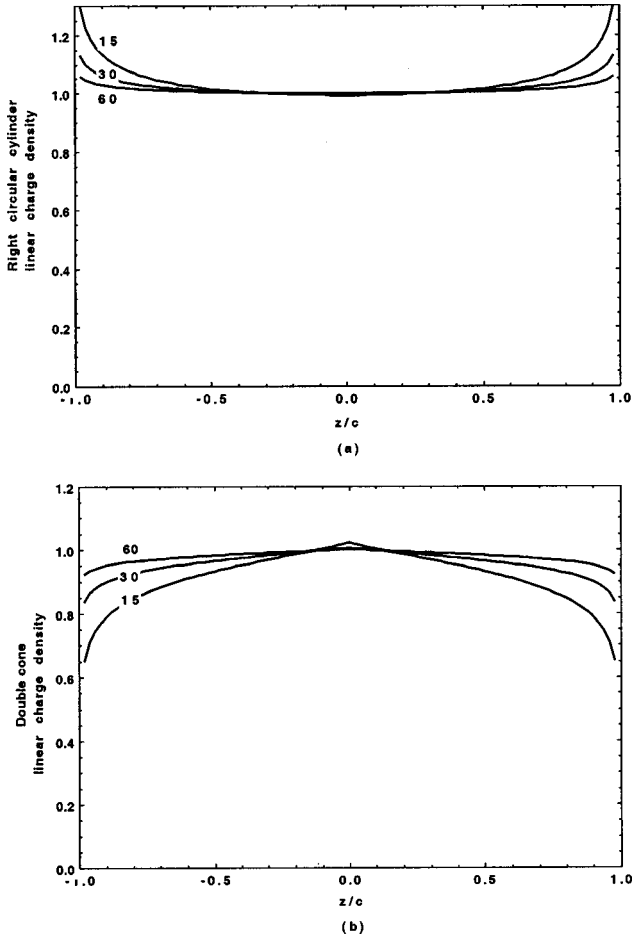

Fig. 5. Behavior of the linear charge density versus z/c with increasing Λ ($\Lambda=15,30,60$) for two different shapes. (a) Right circular cylinder. (b) Double cone.

VI. THIN RIGHT CIRCULAR CONDUCTING CYLINDER (2)

An alternative approach to the problem of the conducting cylinder is an approximation scheme similar to the various numerical methods employed by others. We wish to determine the linear surface charge density on the actual cylinder such that the surface is an equipotential. Since the physical situation is symmetric with respect to the plane $z=0$, the charge density $\lambda(z)$ must be even in z. We expand it in a power series of $N+1$ terms in z^2, with $N+1$ initially unknown coefficients. Since the overall scale of the density is arbitrary, there are really only N coefficients to be determined. We write

$$\lambda(\zeta)=\sum_{k=0}^{N} A_k\zeta^{2k}. \tag{31}$$

The surface charge density is $\sigma(z)=\lambda(z)/2\pi a$. The potential is azimuthally symmetric. We therefore need only the azimuthal average of the Green function $1/|\mathbf{x}-\mathbf{x}'|$. With both the observation point $\mathbf{x}=(a,\ 0,\ z=c\zeta)$ and the source point $\mathbf{x}'=(a\cos 2Q,\ a\sin 2\theta,\ z'=c\zeta')$ on the surface, we find

$$\left\langle \frac{1}{|\mathbf{x}-\mathbf{x}'|}\right\rangle = \frac{2}{\pi c}\int_0^{\pi/2}\frac{d\theta}{\sqrt{(2a/c)^2\sin^2\theta+(\zeta-\zeta')^2}}. \tag{32}$$

In terms of the linear charge density (31) and the averaged Green function (32), the potential becomes

$$\Phi(a,\zeta)=\frac{1}{4\pi\varepsilon_0}\frac{2}{\pi}\int_0^{\pi/2}d\theta\int_0^1 d\zeta'\lambda(\zeta')\times\left[\frac{1}{\sqrt{\alpha^2+(\zeta-\zeta')^2}}+\frac{1}{\sqrt{\alpha^2+(\zeta+\zeta')^2}}\right]. \quad (33)$$

Here we have introduced the quantity $\alpha=2(a/c)\sin\theta$ and exploited the symmetry of $\lambda(\zeta')$ to restrict the ζ' range to (0, 1).

When Φ is expanded in a Taylor series in ζ only even powers occur:

$$\Phi(a,\zeta)=\Phi(0)+\frac{1}{2!}\zeta^2\frac{\partial^2\Phi}{\partial\zeta^2}(0)+\frac{1}{4!}\zeta^4\frac{\partial^4\Phi}{\partial\zeta^4}(0)+\cdots.$$

Here and below we suppress the explicit dependence on a. The longitudinal electric field (times c) is evidently

$$cE_z=-\frac{\partial\Phi}{\partial\zeta}=-\left[\zeta\frac{\partial^2\Phi}{\partial\zeta^2}(0)+\frac{1}{3!}\zeta^3\frac{\partial^4\Phi}{\partial\zeta^4}(0)+\cdots\right]. \quad (34)$$

If we now substitute the power series (31) for $\lambda(\zeta')$ into (33) and require that the first N terms in the expansion (34) vanish (in order to approximate an equipotential on the surface), we obtain N coupled linear equations for the N unknowns, $y_k=A_k/A_0$.

Implicit in the discussion so far is the idea that the ends of the cylinder are unimportant. We must address that issue before proceeding further. If the cylinder is capped by hemispheres of radius a, or a similarly smooth joining, there will be no singularity in the surface charge density at $z=\pm c$. Even with flat plates or a hollow tube, the charge density, though singular (Ref. 13, p. 78) at $\rho=a$, $z=\pm c$, is integrable. The charges within a distance of order a of each end are $\delta Q=O[2\pi a^2\sigma(0)]=O[a\lambda(0)]$.[14] The axial electric field in the central region from the ends is thus estimated to be

$$c|E_z^{(\text{ends})}|=\frac{4\delta Q\zeta}{4\pi\varepsilon_0 c(1-\zeta^2)^2}=O\left(\frac{a}{c}\frac{\lambda(0)}{4\pi\varepsilon_0}\frac{4\zeta}{(1-\zeta^2)^2}\right). \quad (35)$$

The end contribution is $O(a/c)$ compared to (1) or (21), the magnitudes of axial electric field involved in establishing equilibrium on the long cylinder. For $\Lambda>>1$, we clearly have $a/c=2e^{-\Lambda/2}<<1$. For example, $\Lambda=10$ corresponds to $a/c\approx 0.013$; $\Lambda=20$, to $a/c\approx 10^{-4}$. We may safely neglect end effects for $\Lambda>>1$ provided the observation point is not too close to either end. We saw the same sort of restriction in Sec. III.

Now we implement our approximation scheme. We demand

$$\frac{\partial^{2j}\Phi}{\partial\zeta^{2j}}(0)=0 \quad \text{for } j=1,2,3,...,N. \quad (36)$$

In (33) we need

$$\frac{\partial}{\partial\zeta}\left[\frac{1}{\sqrt{\alpha^2+(\zeta\pm\zeta')^2}}\right]=\pm\frac{\partial}{\partial\zeta'}\left[\frac{1}{\sqrt{\alpha^2+(\zeta\pm\zeta')^2}}\right],$$

so that

$$\frac{\partial^{2j}}{\partial\zeta^{2j}}\left[\frac{1}{\sqrt{\alpha^2+(\zeta\pm\zeta')^2}}\right]_{\zeta=0}=\frac{\partial^{2j}}{\partial\zeta'^{2j}}\left[\frac{1}{\sqrt{\alpha^2+\zeta'^2}}\right]. \quad (37)$$

The N constraints (36) are ($j=1,2,3,...,N$)

$$0=\frac{4}{\pi}\int_0^{\pi/2}d\theta\sum_{k=0}^{N}A_k\int_0^1 d\zeta\,\zeta^{2k}\frac{\partial^{2j}}{\partial\zeta^{2j}}\left[\frac{1}{\sqrt{\alpha^2+\zeta^2}}\right]. \quad (38)$$

We define the coefficients in the set of algebraic equations as

$$\beta_{jk}=\frac{4}{\pi(2j)!}\int_0^{\pi/2}d\theta\int_0^1 d\zeta\,\zeta^{2k}\frac{\partial^{2j}}{\partial\zeta^{2j}}\left[\frac{1}{\sqrt{\alpha^2+\zeta^2}}\right]. \quad (39)$$

With $y_k=A_k/A_0$, the N equations of (38) can be written

$$\sum_{k=1}^{N}\beta_{jk}y_k=-\beta_{j0}, \quad j=1,2,3,...,N. \quad (40)$$

The coefficients β_{jk} are evaluated in the Appendix. The results for small a/c are

$$\beta_{jk}=\frac{1}{k-j} \quad \text{for } j\neq k, \quad (41a)$$

$$\beta_{jj}=\Lambda-1\sum_{p=1}^{2j}\frac{1}{p}. \quad (41b)$$

First we look at the large Λ limit. To leading order in Λ, the coupled equations (40) reduce to the uncoupled set,

$$\Lambda y_j=\frac{1}{j}, \quad j=1,2,3,...,N.$$

We may consider the limit of $N\to\infty$ and find the charge density,

$$\lambda(\zeta)=A_0\left[1+\frac{1}{\Lambda}\sum_{j=1}^{\infty}\frac{\zeta^{2j}}{j}\right]=A_0\left[1-\frac{1}{\Lambda}\ln(1-\zeta^2)\right], \quad (42)$$

in agreement with the first-order correction in (26) found above.

To go beyond the asymptotic limit, we may solve the coupled equations by matrix methods. For small N the algebra is manageable by hand. For example, the $N=2$ results for the coefficients are

$$y_1=\frac{2(3\Lambda-14)}{(6\Lambda-25)(\Lambda-3)+6},$$
$$y_2=\frac{3(\Lambda-1)}{(6\Lambda-25)(\Lambda-3)+6}. \quad (43)$$

In Fig. 6 this $N=2$ charge density, correct to order ζ^4 inclusive, is compared with (26), normalized to unity at $z=0$, for $\Lambda=20$. We see that the agreement is good for $|\zeta|<0.7$, but the quartic fails to be singular enough for larger $|\zeta|$. Also shown are the charge densities for $N=5$ and $N=15$, found with the Pascal linear equation tools ''ludcmp'' and ''lubksb'' (Ref. 15, pp. 683, 684) on a Macintosh. Because the results for $N=15$ and (26) are virtually indistinguishable, we plot points for the analytic form to show the agreement. As expected intuitively, the higher the degree N of the polynomial, the better the representation at $|\zeta|$ values near unity.

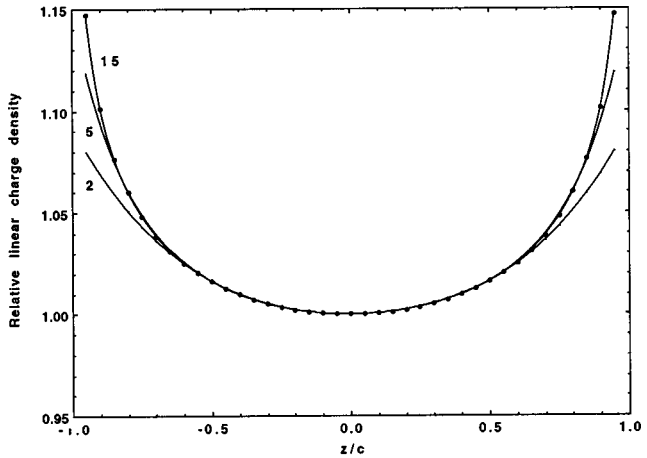

Fig. 6. Comparison of second-order analytic charge density (26) for the right circular cylinder, normalized to unity at $z=0$, (solid points) with $N=2$, 5, and 15 polynomial approximations (continuous curves) for $\Lambda=20$. Note the suppressed zero for the ordinate.

VII. SUMMARY AND CONCLUSIONS

We have revisited the problem of the charge density on a ''wire,'' defined in Sec. II as a very elongated prolate conducting spheroid and more generally in Sec. III, where the issue of the ''unbalanced'' force is resolved. For a conductor of length $2c$ with variable radius $r(z)$ of order a, we give an iteration scheme to generate the linear charge density as a power series in $1/\Lambda$, where $\Lambda\equiv\ln(4c^2/a^2)$. The linear charge density to second order in $1/\Lambda$ inclusive is shown to be

$$\lambda(\zeta)=\lambda_0\left\{1-\frac{1}{\Lambda}\ln\left(\frac{1-\zeta^2}{f(\zeta)}\right)+\frac{1}{\Lambda^2}\left[\left[\ln\left(\frac{1-\zeta^2}{f(\zeta)}\right)\right]^2-I\right]\right\}. \tag{20}$$

where I is given by (19) and $[r(\zeta)/a]^2=f(\zeta)$. [See (8).] For the special case of the right circular cylinder ($f(\zeta)=1$) the integral I can be evaluated analytically. The linear charge density is then

$$\lambda(\zeta)=\lambda_0\left\{1-\frac{1}{\Lambda}\ln(1-\zeta^2)+\frac{1}{\Lambda^2}\left[[\ln(1-\zeta^2)]^2+\frac{1}{2}\left[\ln\left(\frac{1+\zeta}{1-\zeta}\right)\right]^2-\frac{\pi^2}{6}\right]+O(1/\Lambda^3)\right\}. \tag{26}$$

We show that the first-order correction in $\lambda(\zeta)$, though very small for large Λ, produces an electric field *tangent to the surface* of the conductor that just cancels the *tangential* component of the zeroth-order ''unbalanced'' field (1) to give equilibrium to the charge on the surface.

Sections IV and VI treat the practical situation of a conducting right circular cylinder. We compare the result (26) with numerical results in the published literature in Fig. 3. Calculation of the total charge leads to an expression for the capacitance of an isolated long conducting right circular cylinder. A numerical comparison with the results of Smythe[11] for modest $\Lambda(c/a=4,\ 8)$ shows that our result (or equivalently, Vainshtein's[6]) for C is an excellent representation (better than 1%) for $c/a\geqslant 10$ or $\Lambda\geqslant 6$.

In Sec. V we present results obtained by numerical integration for the second-order charge density on long conductors of different shapes. Figure 4 illustrates how the charge density along the conductor varies with shape for finite Λ, while Fig. 5 shows the approach to uniformity with increasing Λ for two different shapes. Even in the limit of infinitesimal a/c, when the charge density is essentially uniform in z and the conductor is virtually a line of charge, the shape leaves its signature in the longitudinal electric field (24).

In Sec. VI a different approach to the right circular cylinder, involving a polynomial approximation in z to the charge density, is presented. With N independent coefficients in the expansion of $\lambda(\zeta)$ to order ζ^{2N}, we demand that the first N terms in a Taylor series in ζ of the tangential electric field at $\rho=a$ vanish. The vanishing of the corresponding derivatives of the potential leads to a set of N inhomogeneous coupled linear algebraic equations for the coefficients in the charge density. To leading order in Λ, the equations become trivial; the limit $N\to\infty$ can be taken; the series can be summed; the first-order analytic result in (26) is obtained. For arbitrary Λ, matrix inversion methods can be used, by hand for small N or by computer for larger N. The results of the polynomial approximation approach are compared with the analytic form (26) in Fig. 6.

It is worth stressing two striking things that emerge here.

(1) The specific behavior of the linear charge density and the fields on the wire depend on its ''primordial'' shape before the limit $a/c<<1$ is taken. The prolate spheroid has a uniform linear charge density $\lambda(z)$ for all aspect ratios and a longitudinal electric field that in the limit approaches (1). For the general azimuthally symmetric conductor, the linear charge density can be expressed as a series in inverse powers of Λ, with the *tangential* electric field vanishing and the asymptotic axial electric field depending on the shape, as given by (24) (which, of course, includes the prolate spheroid as a special case). The right circular cylinder has a nonuniform linear charge density, but no axial electric field because its surface is parallel to the z axis and the surface charge is in equilibrium there.

(2) The second striking thing is the extreme slowness of the approach to uniformity of the linear charge density on the cylinder as a function of c/a. For $c/a=10$, $1/\Lambda=0.1669$; for $c/a\simeq 10^4$, $1/\Lambda=0.050$, only a factor of 3.3 smaller. For $1/\Lambda=0.01$, we need $c/a\simeq 2.6\times 10^{21}$!

In passing we note that the technique of Sec. III (and also Sec. IV) can be applied to the long-wavelength limit of the radar cross-section problem,[4,5,6,7,10] for which one requires the charge density (for calculation of the electric dipole moment) for a potential varying linearly along the length of the cylinder. The relevant charge density is odd in ζ, but otherwise the approaches are identical.

ACKNOWLEDGMENTS

I thank David J. Griffiths for first bringing the problem to my attention in early 1997 and Bruce D. Winstein for reigniting my interest in Spring 1999. George H. Trilling was a most helpful competitor/collaborator in May 1999. As preliminary and incomplete fragments of this paper appeared at that time, he and David Griffiths engaged me in valuable dialogues. I also thank George for a critical reading of this manuscript. Finally, let me thank both referees—one for a meticulous reading of the manuscript and the suggestion of many small but significant improvements in clarity, the other for the observation of other ways of generating numerical approximations to the equilibrium charge density.

APPENDIX

The coefficients β_{jk} in Sec. VI are defined as

$$\beta_{jk}=\frac{4}{\pi(2j)!}\int_0^{\pi/2}d\theta\int_0^1 d\zeta\,\zeta^{2k}\frac{\partial^{2j}}{\partial\zeta^{2j}}\left[\frac{1}{\sqrt{\alpha^2+\zeta^2}}\right], \tag{A1}$$

where $\alpha=(2a/c)\sin\theta$ and $j=1,2,...,N$ while $k=0,1,2,...,N$. In anticipation of choosing $a/c<<1$, we consider the derivative in (A1) in the limit $\alpha\to 0$. Then

$$\lim_{\alpha\to 0}\frac{\partial^{2j}}{\partial\zeta^{2j}}\left[\frac{1}{\sqrt{\alpha^2+\zeta^2}}\right]=\frac{\partial^{2j}}{\partial\zeta^{2j}}\left(\frac{1}{\zeta}\right)=\frac{(2j)!}{\zeta^{2j+1}}. \tag{A2}$$

If we insert this limiting result into (A1), we see that if $k>j$ the ζ integrand is nonsingular. Thus, with the neglect of terms of order $O(a^2/c^2)$ and for $k>j$, we have

$$\beta_{jk}=\frac{4}{\pi}\int_0^{\pi/2}d\theta\int_0^1 d\zeta\,\zeta^{2(k-j)-1}=\frac{1}{k-j}\quad(k>j). \tag{A3}$$

Next consider $k=j$. We have

$$\beta_{jj}=\frac{4}{\pi(2j)!}\int_0^{\pi/2}d\theta\int_0^1 d\zeta\,\zeta^{2j}\frac{\partial^{2j}}{\partial\zeta^{2j}}\left[\frac{1}{\sqrt{\alpha^2+\zeta^2}}\right]. \tag{A4}$$

We integrate by parts twice, recognizing that the odd derivatives of $1/(\alpha^2+\zeta^2)^{1/2}$ vanish at $\zeta=0$ and the even derivatives are finite (for $\alpha\neq 0$), while the qth derivative at $\zeta=1$ is $(-1)^q(q)!$ plus $O(a^2/c^2)$. Neglecting the corrections we then have

$$\beta_{jj}=-\frac{2}{2j}-\frac{2}{2j-1}+\beta_{j-1,j-1}. \tag{A5}$$

Repeated use of this recursion relation gives us

$$\beta_{jj}=-2\sum_{p=3}^{2j}\frac{1}{p}+\beta_{11}. \tag{A6}$$

We now must evaluate β_{11}:

$$\beta_{11}=\frac{4}{\pi}\int_0^{\pi/2}d\theta\int_0^1 d\zeta\,\zeta^2\frac{\partial^2}{\partial\zeta^2}\left[\frac{1}{\sqrt{\alpha^2+\zeta^2}}\right]. \tag{A7}$$

Two integrations by parts yields

$$\beta_{11}=-3+\frac{4}{\pi}\int_0^{\pi/2}d\theta\int_0^1 d\zeta\,\frac{1}{\sqrt{\alpha^2+\zeta^2}}. \tag{A8}$$

The ζ integration gives $\ln[(1+\sqrt{1+\alpha^2})/\alpha]\approx\ln(2/\alpha)=\ln[c/(a\sin\theta)]$. Here we have neglected, as usual, corrections of $O(a^2/c^2)$. The final integral is

$$\begin{aligned}\beta_{11}&=-3+\frac{4}{\pi}\int_0^{\pi/2}d\theta[\ln(c/a)-\ln(\sin\theta)]\\&=-3+2[\ln(c/a)+\ln 2]=\Lambda-2(1+\tfrac{1}{2}).\end{aligned} \tag{A9}$$

We substitute into (A6) to obtain the general result for the diagonal element,

$$\beta_{jj}=\Lambda-2\sum_{p=1}^{2j}\frac{1}{p}. \tag{A10}$$

We now turn to the case of $k<j$. We put $j=k+n$, with $n=1,2,...$. Starting with (A1) instead of (A4), we follow the same procedure of two integrations by parts to obtain the general recursion relation,

$$\begin{aligned}\beta_{k+n,k}=&-\frac{(4k+2n-1)}{(k+n)(2k+2n-1)}\\&+\frac{k(2k-1)}{(k+n)(2k+2n-1)}\beta_{k+n-1,k-1}.\end{aligned} \tag{A11}$$

Now consider the special case $k=0$. The integral (A1) reduces to [neglecting $O(a^2/c^2)$]

$$\begin{aligned}\beta_{n0}&=\frac{4}{\pi(2n)!}\int_0^{\pi/2}d\theta\int_0^1 d\zeta\,\frac{\partial^{2n}}{\partial\zeta^{2n}}\left[\frac{1}{\sqrt{\alpha^2+\zeta^2}}\right]\\&=\frac{4}{\pi(2n)!}\int_0^{\pi/2}d\theta\left[\frac{\partial^{2n-1}}{\partial\zeta^{2n-1}}\left[\frac{1}{\sqrt{\alpha^2+\zeta^2}}\right]\right]_0^1\\&=\frac{4}{\pi(2n)!}\frac{\pi}{2}[-(2n-1)!]=-\frac{1}{n}.\end{aligned} \tag{A12}$$

We now use the recursion relation (A11) to evaluate $\beta_{n+1,1}$:

$$\beta_{n+1,1}=-\frac{1}{(n+1)(2n+1)}\left[2n+3+\frac{1}{n}\right]=-\frac{1}{n}=\beta_{n,0}. \tag{A13}$$

This result suggests that perhaps $\beta_{k+n,k}$ is independent of k. To test this idea we add and subtract $1/n$ to $\beta_{k+n-1,k-1}$ on the right-hand side of (A11). The result is

$$\left(\beta_{k+n,k}+\frac{1}{n}\right)=\frac{k(2k-1)}{(k+n)(2k+2n-1)}\left(\beta_{k+n-1,k-1}+\frac{1}{n}\right). \tag{A14}$$

Beginning at $k=1$ with (A12), we can iterate (A14) successively. The left-hand side is equal to zero for any k. We thus have established that for $j>k$,

$$\beta_{jk}=\frac{1}{k-j}\quad(k<j). \tag{A15}$$

In summary, (A3) and (A15) combine to give, for $k\neq j$,

$$\beta_{jk}=\frac{1}{k-j}, \tag{A16a}$$

while for $k=j$, (A10) is

$$\beta_{jj}=\Lambda-2\sum_{p=1}^{2j}\frac{1}{p}. \tag{A16b}$$

These expressions for the coefficients have corrections of order $O(a^2/c^2)$, appropriately neglected for $\Lambda>>1$.

[1]D. J. Griffiths and Y. Li, ''Charge density on a conducting needle,'' Am. J. Phys. **64**, 706–714 (1996).

[2]R. H. Good, ''Comment on 'Charge density on a conducting needle,' '' Am. J. Phys. **65**, 155–156 (1997).

[3]Mark Andrews, ''Equilibrium charge density on a conducting needle,'' Am. J. Phys. **65**, 846–850 (1997).

[4]P. L. Kapitsa, V. A. Fock, and L. A. Vainshtein, ''Static boundary problems for a hollow cylinder of finite length,'' Zh. Tekh. Fiz. **29**, 1177–1187 (1959) [Sov. Phys. Tech. Phys. **4**, 1077–1087 (1960)].

[5]L. A. Vainshtein, ''Static boundary problems for a hollow cylinder of

finite length. II. Numerical results,'' Zh. Tekh. Fiz. **32**, 1157–1164 (1962) [Sov. Phys. Tech. Phys. **7**, 855–860 (1963)].
[6]L. A. Vainshtein, ''Static boundary problems for a hollow cylinder of finite length. III. Approximate formulas,'' Zh. Tekh. Fiz. **32**, 1165–1173 (1962) [Sov. Phys. Tech. Phys. **7**, 861–866 (1963)].
[7]P. C. Waterman, ''Matrix methods in potential theory and electromagnetic scattering,'' J. Appl. Phys. **50**, 4550–4566 (1979).
[8]W. R. Smythe, *Static and Dynamic Electricity* (McGraw–Hill, New York, 1968), 3rd ed., Sec. 5.02, pp. 123–124.
[9]T. K. Sakar and S. M. Rao, ''An iterative method of solving electrostatic problems,'' IEEE Trans. Antennas Propag. **AP-30** (4), 611–616 (1982).
[10]P. C. Waterman and J. C. Pedersen, ''Scattering by finite wires,'' J. Appl. Phys. **72**, 349–359 (1992).
[11]W. R. Smythe, ''Charged right circular cylinder,'' J. Appl. Phys. **27**, 917–920 (1956); **33**, 2966–2967 (1962).
[12]P. K. Wang, ''Calculation of electrostatic fields surrounding finite circular cylinder conductors,'' IEEE Trans. Antennas Propag. **32**, 956–962 (1984).
[13]J. D. Jackson, *Classical Electrodynamics* (Wiley, New York, 1998), 3rd ed.
[14]A. R. Djordjević, ''Comments on 'Calculation of electrostatic fields surrounding finite circular cylinder conductors,' '' IEEE Trans. Antennas Propag. **33**, 683–684 (1985).
[15]W. H. Press, B. P. Flannery, S. A. Teukolsky, and W. T. Vetterling, *Numerical Recipes, The Art of Scientific Computing* (Cambridge U.P., Cambridge, 1986).

VERSATILE THEORISTS

A hasty investigation of the angular distribution of the neutron beam, performed as soon as the accelerator started functioning, indicated a forward distribution, as expected, but with a minimum at deflection zero. This was reported in a colloquium attended by Oppenheimer, and he immediately gave a learned theoretical explanation of the phenomenon. I listened to it and then said that it was better to check if by chance there was not a lead brick just in front of the target, projecting a shadow. Immediately after the colloquium somebody rushed to check my hypothesis. It was correct.

Emilio Segrè, *A Mind Always in Motion—The Autobiography of Emilio Segrè* (University of California Press, Berkeley, 1993), p. 229.

muonic system in which the muon spends considerable time within the nucleus. The energy value is adjusted upward until the right-hand boundary condition is satisfied (see Fig. 1). The large difference between the seed value and the final energy value (-18.916 vs -10.413 MeV for the $1s$ state) demonstrates the significance of the finite size of the nucleus for muonic atoms.

The fine structure corrections outlined by Tiburzi and Holstein [their Eqs. (16)–(18)] can be easily added to the MATHCAD worksheet (omitted here for the sake of brevity), using traditional numerical algorithms, so that a thorough comparison of theory and experiment can be made.

[a]Electronic mail: frioux@csbsju.edu

[1]B. C. Tiburzi and B. R. Holstein, ''Bound states of a uniform spherical charge distribution-revisited!,'' Am. J. Phys. **68**, 640–648 (2000).
[2]J. Zablotney, ''Energy levels of a charged particle in the field of spherically symmetric uniform charge distribution,'' Am. J. Phys. **43**, 168–172 (1975).
[3]F. Rioux, ''Direct numerical integration of the radial equation,'' Am. J. Phys. **59**, 474–475 (1991).

Comment on ''Charge density on a thin straight wire, revisited,'' by J. D. Jackson [Am. J. Phys. 68 (9), 789–799 (2000)]

O. F. de Alcantara Bonfim and David Griffiths[a)]
Reed College, Portland, Oregon 97202

(Received 5 September 2000; accepted 12 September 2000)

[DOI: 10.1119/1.1326076]

Jackson's paper[1] supports an emerging consensus[2] that the linear charge density on a conducting wire is uniform, in the zero radius limit. This is easily proved for the special case of an ellipsoid, but Jackson demonstrates that it holds regardless of shape. This conclusion is so counterintuitive that we decided to reexamine the original numerical studies,[3] based on discrete charge distributions, that appeared to confirm the more plausible hypothesis that the charge accumulates preferentially near the ends.

We place N charges at equal spacing on the interval $0<x\leqslant 1$:

$$\begin{aligned} &q_1 \quad \text{at } x_1=1/N,\\ &q_2 \quad \text{at } x_2=2/N,\\ &\cdots\\ &q_n \quad \text{at } x_n=n/N,\\ &\cdots\\ &q_N \quad \text{at } x_N=1 \end{aligned} \tag{1}$$

(and equal charges at the corresponding points on $-1\leqslant x<0$), together with a single charge q_0 at $x_0=0$. We then adjust the charges so that the Coulomb force on each of them except q_N (which is subject to an extra confining force) is zero:

$$\sum_{j=1}^{N}\frac{q_j}{(n+j)^2}+\frac{q_0}{n^2}+\sum_{j=1}^{n-1}\frac{q_j}{(n-j)^2}-\sum_{j=n+1}^{N}\frac{q_j}{(j-n)^2} =0 \quad (n=1,2,\ldots,N-1), \tag{2}$$

subject to the constraint

$$q_0+2\sum_{n=1}^{N}q_n=1 \tag{3}$$

(the scaled total charge on the wire). This does not determine the charge at the center—the force on q_0 is automatically zero, by symmetry. To ensure continuity we choose $q_0=q_1$. What remains is a set of N linear equations for the N unknown charges.

Griffiths and Li[2] solved this system numerically for N up to 100, and persuaded themselves that the linear charge density was approaching a nontrivial limiting form—fairly flat in the center, but with spikes at the ends ($x=\pm 1$). They were seduced by extraordinarily slow convergence as N

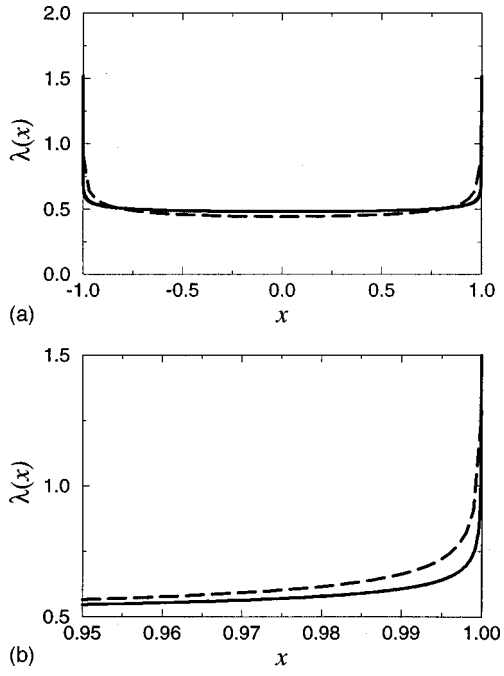

Fig. 1. Linear charge density on a needle, as a function of position. The calculation was done using $2N+1$ point charges equally spaced on the interval from -1 to $+1$, and requiring that the net force on each charge (except the end two) vanish. The total charge on the needle is 1. (a) Solid line: $N=16\,384$; dashed line: $N=32$. (b) Expanded view of the right end; this time the dashed line is $N=1024$.

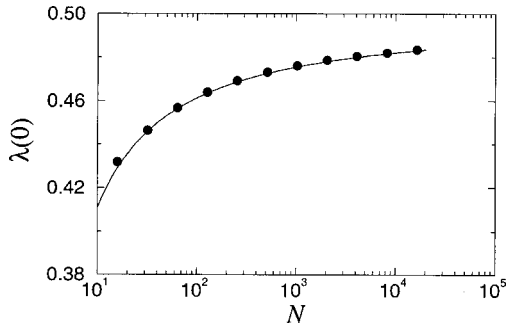

Fig. 2. Charge density at the center of the needle, as a function of N. Dots represent the numerical results. The solid line is the best fit of the form $\lambda(0)=P_1+P_2/\ln N+P_3/(\ln N)^2$ (for N ranging from 32 to 16 384), which occurs for $P_1=0.500$, $P_2=-0.152$, and $P_3=-0.123$. Evidently $\lambda(0)$ approaches the uniform density value of 0.5, as N increases.

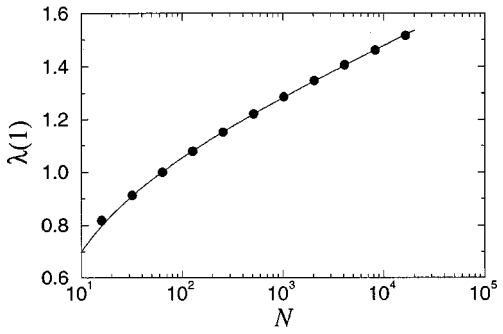

Fig. 3. Charge density at the ends of the needle ($x=\pm1$), as a function of N. Dots represent the numerical results. The solid line is the best fit of the form $\lambda(1)=[Q_1+Q_2/\ln N+Q_3/(\ln N)^2]\ln N$, which occurs for $Q_1=0.0719$, $Q_2=0.912$, and $Q_3=-0.874$. Evidently $\lambda(\pm1)$ diverges as N increases.

$\rightarrow\infty$, as we can see from Fig. 1, which extends the calculation out to $N=16\,384$: As N increases, the charge density approaches 1/2, except at the very ends, which occupy a decreasing portion of the length and contain a diminishing fraction of the total charge.

In Fig. 2 we plot the charge density at the center ($\lambda(0)=Nq_0$) as a function of N, to demonstrate the (painfully slow) approach to 0.5. Jackson shows that the natural expansion parameter is Λ^{-1}, where $\Lambda\equiv\ln(4c^2/a^2)$, with $2c$ the length of the wire and a its characteristic ''radius,'' and he suggests that for the discrete model this translates to $\Lambda\sim2\ln N$. In Fig. 2 the solid line is a best fit of the form

$$\lambda(0)=P_1+\frac{P_2}{\ln N}+\frac{P_3}{(\ln N)^2}; \tag{4}$$

for our data (with N ranging from 32 to 16 384) $P_1=0.500$, $P_2=-0.152$, and $P_3=-0.123$.

In Fig. 3 we plot the charge density at the ends of the wire ($\lambda(1)=Nq_N$), as a function of N. It seems clear that this quantity increases without limit—in fact, our data are well represented by the functional form

$$\lambda(1)=\left[Q_1+\frac{Q_2}{\ln N}+\frac{Q_3}{(\ln N)^2}\right]\ln N, \tag{5}$$

with $Q_1=0.0719$, $Q_2=0.912$, and $Q_3=-0.874$ (solid line). Nevertheless, these ''rabbit ears'' in $\lambda(x)$ are of decreasing significance as $N\rightarrow\infty$, in the sense that they occupy a diminishing portion of the total length and contain a smaller and smaller fraction of the total charge.

ACKNOWLEDGMENT

We thank Nicholas Wheeler for illuminating discussions of this problem.

[a]Electronic mail: Griffith@reed.edu

[1]J. D. Jackson, ''Charge density on a thin straight wire, revisited,'' Am. J. Phys. **68**, 789–799 (2000).

[2]R. H. Good, ''Comment on 'Charge density on a conducting needle,' '' Am. J. Phys. **65**, 155–156 (1997); Mark Andrews, ''Equilibrium charge density on a conducting needle,'' *ibid.* **65**, 846–850 (1997); Nicholas Wheeler, ''Construction and applications of the fractional calculus'' (unpublished).

[3]D. J. Griffiths and Ye Li, ''Charge density on a conducting needle,'' Am. J. Phys. **64**, 706–714 (1996).

PREPARATION?

Gibbs began his lectures on thermodynamics with the Carnot cycle, which he always got wrong. After getting thoroughly mixed up he concluded the first lecture with an apology, and in the second lecture he gave it letter perfect. It was in this way he introduced entropy, rather than in the formal way in the ''Heterogeneous Substances''.

E. B. Wilson, a student of J. Willard Gibbs, as quoted by Clifford Truesdell in J. Serrin (editor), *New Perspectives in Thermodynamics* (Springer, New York, 1986), p. 107.